

Compact Spatial Correlation Formula for MIMO in Factory Environment

KY Leng¹, Kei Sakaguchi², and Kiyomichi Araki³, Non-members

ABSTRACT

Multiple-Input Multiple-Output (MIMO) transmission scheme is considered as a promised technology for future wireless communication since it offers significant increases in data throughput and link range without additional bandwidth or transmitted power. However, the MIMO channel capacity is severely degraded by the correlation between individual sub-channels of its channel matrix. Hence, in system simulations, the correlation should be taken into account. Since the conventional method such as the extended one ring and double ring scatterers model require the knowledge of each multipath components, it is obvious that a simpler model, but accurate enough, should be proposed to reduce the complexity and the calculation time of the model. In this paper, we propose a compact spatial correlation formula that can be used to calculate the channel capacity of MIMO system in 950 MHz band at factory environment. The validity of the proposed model also holds for other environments and frequency bands. With the proposed model, we need to know only three important parameters, such as antenna size, antenna separation, and Rician K factor to generate the spatial correlation of the channel.

Keywords: MIMO Channel Capacity, Spatial Correlation, K-factor, Line-of-Sight Component

1. INTRODUCTION

In recent years, Multiple-Input Multiple-Output (MIMO) wireless communication techniques have attracted strong attention in research and development due to their potential benefit in spectral efficiency, throughput and quality of service. However, it demands a great effort to test the performance of a system, such as the real behavior of protocols and network performance, using MIMO technology by a test-bed. Hence, a high level protocol simulation is preferred, especially for Wireless Sensor Networks (WSN), with hundreds or thousands of sensor nodes, which use MIMO as a core technology for data transmission [1-3].

Manuscript received on May 19, 2009 ; revised on April 4, 2010.

^{1,2,3} The authors are with Tokyo Institute of Technology, Tokyo, 152-8552 Japan. E-mail: leng@mobile.ee.titech.ac.jp, kei@mobile.ee.titech.ac.jp and araki@mobile.ee.titech.ac.jp

Since the correlation effect between individual sub-channels of the MIMO channel matrix can degrade the performance of MIMO, the correlation effect should be taken into account in the system simulation. To our knowledge, until now, when MIMO system simulation are performed, the spatial correlation is included by means of measured data, or based on a ray-tracing method or by using a one ring or double ring scatterers model or Salz-Winters spatial correlation model. Some of these approaches are difficult to carry, especially for WSN, since the MIMO channel statistics are represented by a large number of parameters due to its multipath components; and others lack of generality.

Note that, for WSN, the design goals are focused on energy saving, traffic and environment adaptability. It is mainly used for data collection and event control. The maximum transmitted power for such narrow band and small coverage is about 5 dBm. For mobile communication, the design goals are mobility and high speed transmission. It is mainly used for voice and data communication systems. The maximum transmitted power for such wider bands and larger coverage is about 30 dBm to 33 dBm. The main differences between WSN and cellular communication are the initial motivation keys of this paper.

In this paper, a simplified spatial correlation model is introduced for WSN using MIMO, then extended to cover MIMO in the general case. Moreover, this paper is an extended version of our work in [7] which focuses on the development of a pathloss model for WSN using MIMO in a factory environment. We intend to remain with the factory environment condition until the formula is derived.

Using test-bed to measure data in a real environment demands a lot of effort and time. In this paper, we use a ray-tracing method to arrive at the raw data. This method is expected to provide data close to the real measurement.

In [4, 6], the correlation model is a function of the antenna separation and the antenna size only. In our model, we introduce a Rician K factor, which is a ratio between the Line of Sight (LOS) component and diffused multipath components. Unlike [5], which specifies the correlation model and channel matrix with the number of scatterers around transmitter and receiver, we arrive at a model free from specifying multipath components. Hence, we reduce the computational resource and time.

The rest of this paper is organized as follows.

Section 2 presents a review and updated version of our work in [7], and the evaluation of the proposed pathloss model is presented in Section 3. Section 4 proposes a MIMO channel model using the outcome from the proposed pathloss and spatial correlation formula, and the validation of this spatial correlation formula is evaluated in Section 5. Finally, the conclusion is discussed in Section 6.

2. PATHLOSS MODEL AND SPATIAL CORRELATION FORMULA

The objective of our research in [7] aims to develop a pathloss model for WSN using MIMO technology in factory environments. The pathloss model is designed to work at 950 MHz band, whereas the spatial correlation is designed for two transmitted (Tx) and two received (Rx) antennas. These models are designed for three basic environments, named Roof-to-Roof (RR), Roof-to-Ground (RG) and Ground-to-Ground (GG). Since these correlations are assumed independent [8], and in WSN, all sensor nodes are assumed fixed (no temporal correlation) and the propagation channel is narrowband (no spectral correlation), we will consider only the effect of spatial correlation. Unless otherwise stated, the word correlation refers to spatial correlation for the rest of this paper.

In this paper, process #5 and #6 in [7] Section 3 are repeated. However, we do not fix the antenna spacing $D = \frac{1}{2}\lambda$ as before. On the other hand, we regenerate and recalculate our spatial correlation coefficients (for RR, RG and GG environment at both Tx and Rx side) for D ranging from 0.3λ to 3λ with a step of 0.1λ . For each antenna spacing, we recalculate all these spatial correlation coefficients in all possible Tx-Rx distances d .

2.1 Kronecker model validity

In order to verify the validity of the Kronecker model as stated in [9, 10], it is necessary to only verify whether the Direction-of-Arrival (DoA) spectral and the Direction-of-Departure (DoD) spectral are independent or not.

Figure. 1 shows the spatial correlation coefficient at Tx and Rx side versus the distance where $D = \frac{1}{2}\lambda$ and antenna size at both sides $N = 2$ in RR environment. The reason why we selected RR environment is because this environment has less numbers of multipaths compared to the other two environments. So if the Kronecker model is valid in this environment, it must be valid in the other two as well.

For a factory environment as shown in [7], it seems that there are so many reflected and diffracted objects in between Tx and Rx antennas. If this is true, we can say directly that DoD and DoA spectral are independent. However, we do not conclude this statement based on geometry alone. To be transparent, we mark all the spatial correlations that are smaller than 0.1

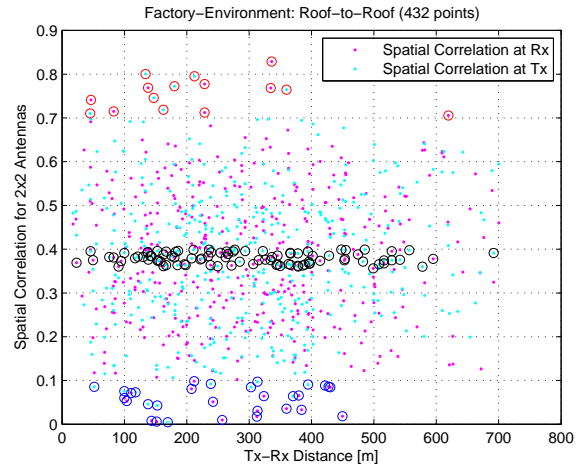


Fig. 1: Distribution of spatial correlation coefficient vs distance

(blue circle), then in between its mean value ± 0.02 (black circle), and all the value that are bigger than 0.7 (red circle). See also Fig. 1. Finally, we verify the corresponding position of each spatial correlation point with the factory map to see the relationship between these correlation values, and building heights.

As expected, there is no correlation between these stated relationships because we expect in general that for the RR environment the correlation between sub-channel must be close to 1 since there are so little multipath components which interfere with the LOS components. However, as we can see from Fig. 1 there are so many points that are smaller than 1 and some of them are even close to 0. When we check the geometric position of those points that are close to 0 (smaller than 0.1), we found that, for some Tx-Rx pair, both positions (height of Tx and Rx) are high from the ground, and on some, Tx is high but Rx is low (the lowest height for RR environment is 4 m), and vice-versa. We can conclude that the spatial correlation for this factory environment is independent of building height.

Moreover, from this figure, we can see that the spatial correlation coefficients at both side seem to be randomly distributed in all distance values. This figure also shown that the mean value of the spatial correlation in each distance block seem to be constant over the propagation distance. Normally, the mean value of the spatial correlation changes over distance, however, it does not change here. This is because of the propagation distance of our model is small (less than 1 km for microcell environment). We can also say that, for a given Tx and Tx-Rx distance, the correlation at Rx side can have value in between 0 and 1 which mean the DoA and DoD spectral are not the same. In other word, DoA and DoD spectral are independent for RR environment. With similar reasons, DoA and DoD spectral are independent for RG and

GG environment as well.

We can conclude that the Kronecker model is valid for this factory environment as well as other environments of the same kind.

2.2 Spatial correlation distribution

In the previous Subsection, we found that the spatial correlation values are randomly distributed for a given Tx-Rx distance d and seem to be the same for different value of d . It is better to represent these spatial correlation values by a statistical means.

Unlike [7], this time, we evaluate the performance of the fitted distribution by means of Maximum Likelihood Estimation (MLE); and the candidate distribution function to be chosen for this time are Gaussian, Rayleigh, and Rician since the Rician K factor is about 0 (mean Rician become Rayleigh) in [7].

From Fig. 2(a), we can see that the Maximum Likelihood Value (MLV) using Rician distribution is always higher or equal to the MLV using Gaussian and Rayleigh. In some cases, the MLV using Rayleigh is higher than the MLV using Gaussian. However, we can say in general that the MLV using Gaussian are very close to that using Rician.

From Fig. 2(b), we can see that the standard deviation in Gaussian case is more stable than that in Rician, moreover, from Fig. 2(c), the variation of the mean value in Gaussian case can be represented by a modified zero-order Bessel function of the first kind, which is more convenient to represent than the variation of V value in Rician case. See also Fig. 3 where the variation of the mean (or median for Gaussian distribution) value of both correlation at Tx and Rx side are plotted with different Rician K values. We will discuss more about this figure in the Section 4.

Based on these reasons, Gaussian distribution is chosen with the condition that the spatial correlations generated using Gaussian are in between the values 0 and 1. The work in [7] also confirms this final selection.

Since the antenna separation $D = \frac{1}{2}\lambda$ is far enough to ignore the mutual coupling effect between the nearby antenna, we can use Fig. 2(c) to get the spatial correlation for the other antennas as well. For example, in a 4×4 MIMO system, the correlation matrix \mathfrak{R} is formed by its component \mathfrak{R}_{ij} where $i, j = 1, 2, 3$, and 4. By symmetry and the property of the correlation matrix, we need to know only \mathfrak{R}_{12} which corresponds to $D_{12} = \frac{1}{2}\lambda$, \mathfrak{R}_{13} which corresponds to $D_{13} = \frac{2}{2}\lambda = \lambda$, and \mathfrak{R}_{14} which corresponds to $D_{14} = \frac{3}{2}\lambda$.

Based on this consideration, and that it is more than enough at the present time for WSN to use at maximum 4 antennas at each node, we will show only the spatial correlation for the 4×4 MIMO system. Moreover, as the Kronecker model is selected as a proper correlation model to be used, we will show directly the square root of the corresponding spatial

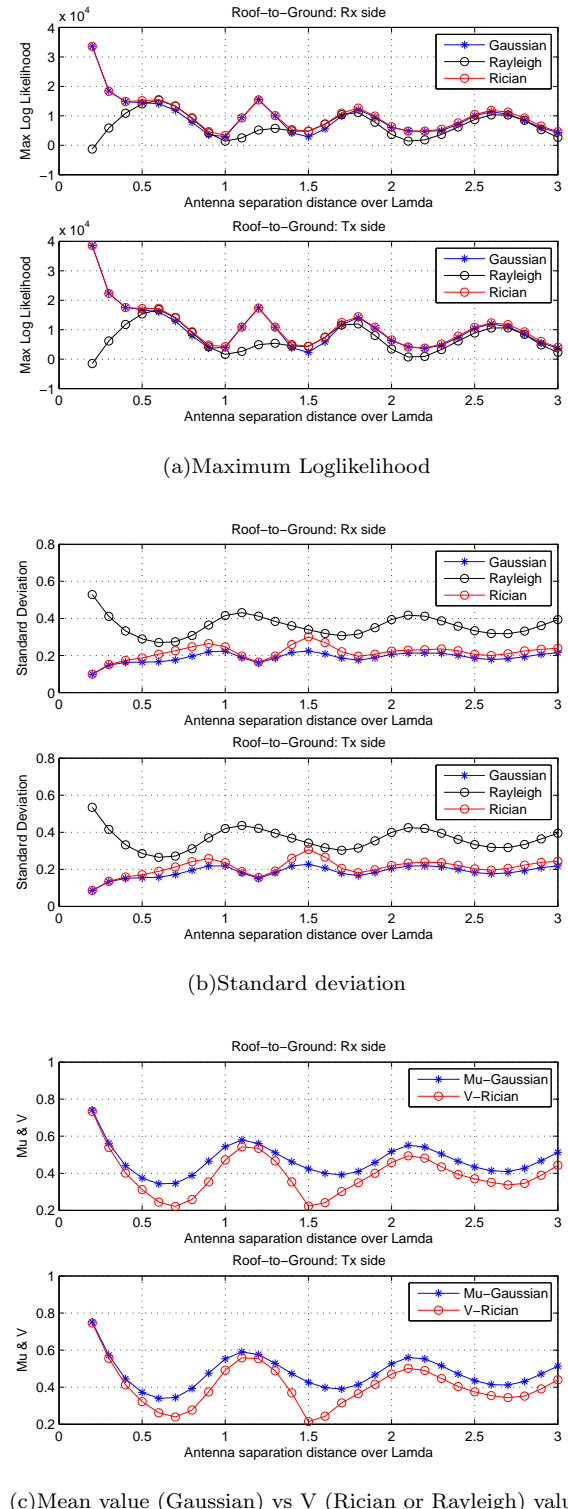


Fig.2: Fitting results from Roof-to-Ground environment Data

correlation at Tx and Rx in RR, RG, and GG environment as listed below.

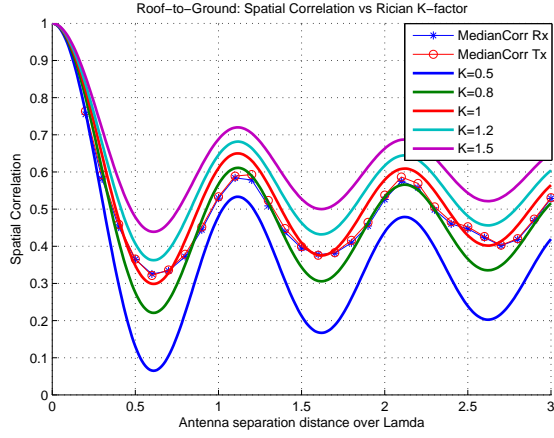


Fig.3: Spatial correlation coefficient vs distance

$$\mathfrak{R}_{Tx_{RR}}^{\frac{1}{2}} = \begin{bmatrix} 0.9430 & 0.1412 & 0.2611 & 0.1502 \\ 0.1412 & 0.9442 & 0.1426 & 0.2611 \\ 0.2611 & 0.1426 & 0.9442 & 0.1412 \\ 0.1502 & 0.2611 & 0.1412 & 0.9430 \end{bmatrix} \quad (1)$$

$$\mathfrak{R}_{Rx_{RR}}^{\frac{1}{2}} = \begin{bmatrix} 0.9371 & 0.1460 & 0.2798 & 0.1491 \\ 0.1460 & 0.9375 & 0.1465 & 0.2798 \\ 0.2798 & 0.1465 & 0.9375 & 0.1460 \\ 0.1491 & 0.2798 & 0.1460 & 0.9371 \end{bmatrix} \quad (2)$$

$$\mathfrak{R}_{Tx_{RG}}^{\frac{1}{2}} = \begin{bmatrix} 0.9412 & 0.1401 & 0.2530 & 0.1745 \\ 0.1401 & 0.9462 & 0.1450 & 0.2530 \\ 0.2530 & 0.1450 & 0.9462 & 0.1401 \\ 0.1745 & 0.2530 & 0.1401 & 0.9412 \end{bmatrix} \quad (3)$$

$$\mathfrak{R}_{Rx_{RG}}^{\frac{1}{2}} = \begin{bmatrix} 0.9426 & 0.1402 & 0.2473 & 0.1750 \\ 0.1402 & 0.9477 & 0.1450 & 0.2473 \\ 0.2473 & 0.1450 & 0.9477 & 0.1402 \\ 0.1750 & 0.2473 & 0.1402 & 0.9426 \end{bmatrix} \quad (4)$$

$$\mathfrak{R}_{Tx_{GG}}^{\frac{1}{2}} = \begin{bmatrix} 0.9348 & 0.1463 & 0.2855 & 0.1527 \\ 0.1463 & 0.9356 & 0.1474 & 0.2855 \\ 0.2855 & 0.1474 & 0.9356 & 0.1463 \\ 0.1527 & 0.2855 & 0.1463 & 0.9348 \end{bmatrix} \quad (5)$$

$$\mathfrak{R}_{Rx_{GG}}^{\frac{1}{2}} = \begin{bmatrix} 0.9376 & 0.1460 & 0.2760 & 0.1528 \\ 0.1460 & 0.9386 & 0.1471 & 0.2760 \\ 0.2760 & 0.1471 & 0.9386 & 0.1460 \\ 0.1528 & 0.2760 & 0.1460 & 0.9376 \end{bmatrix} \quad (6)$$

3. VALIDATION OF THE PATHLOSS MODEL

In our previous work [7], the proposed pathloss model was verified with the free space and d^{-4} model. In this paper, we compared our model (RG environment for a fair comparison with other models) with

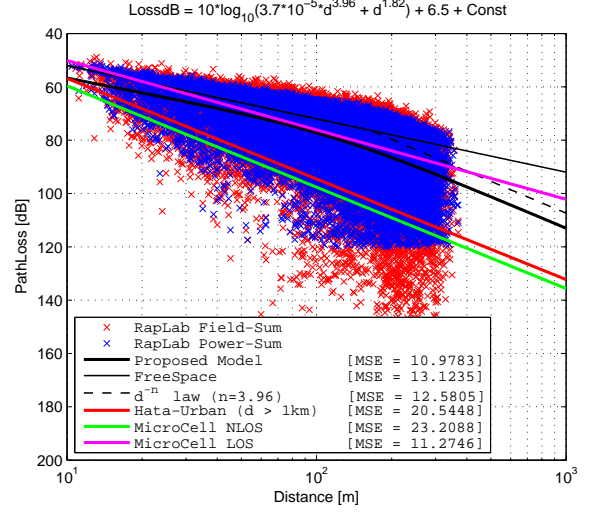


Fig.4: Roof-to-Ground pathloss in factory environment

the Hata model for urban areas and the COST 231 Walfish-Ikegami in Line of Sight (LOS) and None Line of Sight (NLOS) microcell. Note that our pathloss model aims to improve the accuracy of the high level protocol simulation of WSN as mentioned in [2] whereas Hata model and COST 231 model are mainly used in cellular communication systems [11, 12].

In order to see more clearly the difference between these models, we decide to use the Mean Square Error (MSE) value to judge which one is the best representation of the real pathloss in factory environments as shown in Fig. 4.

Note that Hata model for Urban area (Hata-Urban) is valid for distance between 1 km till 20 km. However, we want to know only how far the performance of this model is from the proposed model. From this figure, we see that the best fit to the raw data is our proposed model, the next good one is COST 231 Walfish-Ikegami for microcell LOS (Microcell LOS), and the third good one is d^{-n} law with pathloss exponent $n = 3.96$.

From these observations, we can say that this RG factory environment can be considered as microcell LOS environment and is desirable to represent this pathloss by d^{-n} law since this law considers the pathloss in two different situations called pathloss before and after break point distance d_b . It is more desirable to represent this pathloss by our model since our model considers a smooth transition between the two environment before and after d_b . See also [7].

The formulas and parameters used in this paper are taken from [11, 12]. With Base Station (BS) antenna height $h_B = 12.5$ m, Mobile Station (MS) antenna height $h_M = 1.5$ m, and other necessary parameter as listed in [12], the Hata-Urban, the microcell NLOS and LOS pathloss are respectively simplified

to:

$$\begin{aligned} L_{dB_{NLOS}} &= -58.5 + 37.7 \log_{10} d \\ &\quad + 26.1 \log_{10} f_c \end{aligned} \quad (7)$$

$$\begin{aligned} L_{dB_{NLOS}} &= -55.9 + 38 \log_{10} d \\ &\quad + (24.5 + \frac{1.5}{925} f_c) \log_{10} f_c \end{aligned} \quad (8)$$

$$L_{dBLOS} = -35.4 + 26 \log_{10} d + 20 \log_{10} f_c \quad (9)$$

where f_c is the operating frequency in MHz, and d is the distance between Tx and Rx in m. In those formulae, d is at least 20 m.

With the parameters stated above, the break point distance d_b , measured in [m], can be calculated using the following equation.

$$d_b = \frac{4h_M h_B f_c}{300} \quad (10)$$

This implies $d_b = 237.5$ m. If $n = 4$ was chosen, the resulting MSE of d^{-n} law is 13.0411. In Fig. 4, $d_b = \frac{1}{\sqrt{C}} = 164.4$ m was chosen, where $C = 3.7 \times 10^{-5}$ is the coefficients in the proposed model in [7]. With this setting and $n = 3.96$ was chosen, the MSE of d^{-n} law is now reduced to 12.58, which means that the propose model is flexible and reflects the behaviors of the environment than any existing models.

Using the method in [7], Section 4, it is very easy to verify that the above formulae are special cases of our proposed model. We can conclude that the proposed pathloss model is valid for any environment and frequency band with so little modification of its coefficients.

4. MIMO CHANNEL MODEL AND FINAL PATHLOSS MODEL RESULT

For a fixed linear channel matrix H with zero-mean additive white Gaussian noise, and when the transmitted signal vector is composed of statically independent equal power components each with a Gaussian distribution, the MIMO channel capacity can be denoted by [5, 13] as:

$$C_{MIMO} = \log_2 \left[\det \left[I_N + \frac{\rho}{M} H H^H \right] \right] \quad (11)$$

where $\det[\cdot]$ denotes the determinant operator, $[\cdot]^H$ denotes Hermitian transpose of a matrix, M is the number of transmitting antennas, N is the number of receiving antennas, H is $N \times M$ normalized channel matrix between the transmitter (Tx) and receiver (Rx), ρ is the Signal-to-Noise Ratio (SNR) per Rx antenna, and I_N is $N \times N$ identity matrix.

For a correlated channel, let \mathfrak{R}_{Tx} and \mathfrak{R}_{Rx} be the correlation matrix at Transmitter side (Tx) and Receiver side (Rx) respectively. So, the normalized channel matrix can be generated by [9] as:

$$H = \mathfrak{R}_{Rx}^{\frac{1}{2}} U \mathfrak{R}_{Tx}^{\frac{1}{2}} \quad (12)$$

Table 1: Rician K factor in different environment

Environment	Rician K factor
Roof-to-Roof (RR)	0.85
Roof-to-Ground (RG)	0.80
Ground-to-Ground (GG)	0.90
Factory (RR, RG, GG)	0.85

where U is a stochastic matrix with i.i.d. complex Gaussian zero-mean unit variance elements. Similarly, for an uncorrelated channel, the channel matrix H can be defined as:

$$H = U \quad (13)$$

In this paper, since the result from ray-tracing shows that the spatial correlation at the Tx side are very close to that at the Rx side, we will assume that $\mathfrak{R} = \mathfrak{R}_{Tx} = \mathfrak{R}_{Rx}$. The validity of this assumption will be checked in Section 5. The correlation matrix at Tx or Rx side, can be denoted as \mathfrak{R} , is defined (when $i \neq j$), based on [5, 7], as:

$$\mathfrak{R}_{ij} = \frac{J_0(\frac{2\pi D_{ij}}{\lambda}) + K}{(1 + K)} \quad (14)$$

where J_0 is zeroth-order Bessel function of the first kind, K is the Rician factor of the working environment, D_{ij} is the distance between antenna i and antenna j at each side (Tx or Rx side), and λ is the wavelength which correspond to the operating frequency. In order to get the correlation matrix, we need only the basic information such as antenna size at Tx or Rx side, antenna spacing, and Rician K factor of the environment. The knowledge of multipath components is not required.

From the result in Fig. 3, the K value corresponding to RG environment is in between 0.5 and 1. However, on average, K takes the value of 0.8. This result also means that this environment can be considered as a LOS microcell which conform with the result in Section 3. Since the variation of K value is small around its mean value, we decided to represent the corresponding environment by only one K value. Note that in [5], K is initially used to characterize only the environment between each antenna pair. Later on, they admit that the Rician factor for each antenna pair is the same, so it is obvious to use one K value for one environment. Table 1 shows the Rician K factor in RR, RG, and GG environment as well as in the whole factory environment.

If the upper bound of MIMO channel capacity is needed, Jensen inequality is preferred and this upper bound capacity is defined, based on [13] and the inequality & concavity of $\log \det$ function [14], as:

$$\begin{aligned} \langle C_{MIMO} \rangle &\leq \log_2 \left[\det \left[I_N + \frac{\rho}{M} \langle H H^H \rangle \right] \right] \\ &= \log_2 \left[\det \left[I_N + \frac{\rho}{M} \mathfrak{R}_{Rx} N I_N \right] \right] \end{aligned} \quad (15)$$

Table 2: Final proposed pathloss model for factory environment at 950 MHz band

$L_{dB} = 10\log_{10}(Cd^{n_2} + Bd^{n_1}) + A + Const$ $+ (X_\sigma - \sigma\sqrt{\pi/2})$ $\sigma = bd + a$ $\Re = \Re_{Tx} = \Re_{Rx} = N(\mu_0, \sigma_0^2)$ $\mu_0 = \frac{J_0(\frac{2\pi D}{\lambda}) + K}{(1+K)}$			
Parameters	RR	RG	GG
n_2	3.73	3.96	6.15
n_1	1.77	1.82	2.45
C	7×10^{-5}	3.7×10^{-5}	6×10^{-7}
B	1	1	1
A	5	6.5	-7
b	0.00497	0.0232	0.0520
a	7.104	7.440	19.912
σ_0	0.2	0.2	0.2
K	0.85	0.85	0.85
$Const$	32	32	32

where $\langle \cdot \rangle$ is the expectation over the channel matrix.

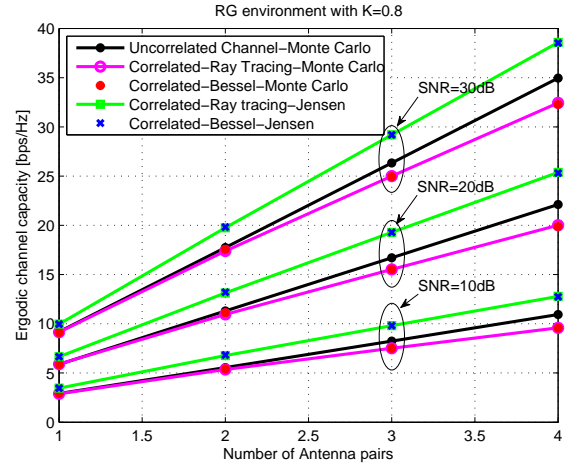
For the reason of simplicity, we will use the upper bound of the MIMO ergodic channel capacity in the design and analysis of the system. The simplified version of the MIMO channel capacity can be rewritten with a very simple expression as:

$$\langle C_{MIMO} \rangle \cong \log_2 \left[\det \left[I_N + \frac{\rho}{M} \Re_{Rx} N I_N \right] \right] \quad (16)$$

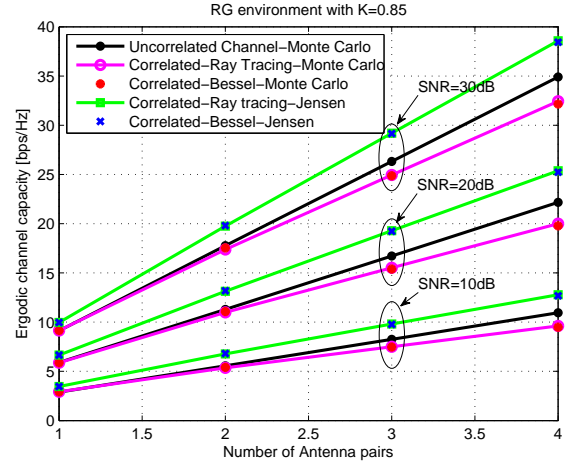
Finally, the summary of the proposed pathloss model is presented in Table 2 for future use.

The parameters using in this Table are defined as follows: A, B , and C are the coefficients that define the characteristic of the environment, n_1 and n_2 define the pathloss exponent in the zone before and after break point distance d_b respectively, d is the distance between Tx and Rx, and D is the separation between two antennas. $Const$ is the system loss constant which is defined as $20\log_{10}(\frac{4\pi f}{c})$ where f is the operating frequency in Hz, and c is the speed of light in vacuum (3×10^8 m/s). For the operating frequency of 950 MHz, $Const = 32$ dB. In some case, n_2, n_1, A, B , and C can be functions of f as well. X_σ characterizes the loss of the received surrounding environment (shadowing) [7, 15, 16]. It is a Rayleigh random variable with standard deviation σ ($\sigma = bd + a$, where a , and b are the coefficients defined the characteristic of the environment).

Note that, this model is valid for other frequency band and environment, but the coefficients used in this Table are valid for the frequency band of 950 MHz and factory environment where the average building height is 8.4 m (or the average antenna height on the roof is 13.4 m) with the standard deviation of 6.38 m.



(a) Roof-to-Ground environment with $K=0.80$



(b) Roof-to-Ground environment with $K=0.85$

Fig.5: Channel capacity vs antenna size

5. EVALUATION OF THE SPATIAL CORRELATION FORMULA

In order to evaluate the validity of the proposed spatial correlation formula in Section 4, we decide to plot the ergodic channel capacity of a MIMO system with different antenna pairs and SNR. Since Rician K factor for RR, RG, and GG environment are different, we decided to plot $K = 0.80$ and $K = 0.85$ with RG environment data in Fig. 5. Note that $K = 0.80$ is the optimum value for RG environment only, whereas $K = 0.85$ is the average value among RR, RG, and GG. This value defines the characteristic of factory environment.

In this figure, the graph named ‘Uncorrelated Channel-Monte Carlo’ is generated using Equ. 11 and Equ. 13; whereas the graph named ‘Correlated-Ray Tracing-Monte Carlo’ is generated using Equ. 11, Equ. 12, Equ. 3, and Equ. 4; and the graph named ‘Correlated-Bessel-Monte Carlo’ is generated using Equ. 11, Equ. 12, and Equ. 14. Similarly, graph

named ‘Correlated-Ray Tracing-Jensen’ is generated using Equ. 16, and Equ. 4; and the graph named ‘Correlated-Bessel-Jensen’ is generated using Equ. 16, and Equ. 14.

From this figure, we see that the graph ‘Correlated-Bessel-Monte Carlo’ gives a result close to ‘Correlated-Ray Tracing-Monte Carlo’ in any SNR, antenna pair and K value. Similarly, the graph ‘Correlated-Bessel-Jensen’ gives a result close to ‘Correlated-Ray Tracing-Jensen’. Moreover, the graphs using Bessel function are closer to the graphs using Ray-tracing data when $K = 0.80$ than $K = 0.85$. However, the differences are little.

From this figure, we can also see the effect of spatial correlation on the MIMO channel capacity. Normally, the channel capacity of an uncorrelated channel increases linearly with the antenna size, but by adding the correlation effect to the channel, the MIMO capacity decreases and the difference between these two become larger and larger. If we increase the antenna size, the result for the MIMO correlated channel capacity does not increase linearly with the antenna size. For 2×2 MIMO, this difference can be negligible.

We can conclude that instead of using data from Ray-tracing (Equ. 1 to Equ. 6) which demands a lot of efforts, Equ. 14 can be used to generate the correlation matrix \mathfrak{R} as well as correlated channel matrix H with a very simple calculation complexity, and yet good accuracy. Since an environment can always be modeled by a Rician K factor, we also can generate the correlation matrix without complexity and loss of precision using this compact spatial correlation formula (Equ. 14). This statement holds for other environments and frequencies as well.

6. CONCLUSIONS

In this paper, a complete pathloss model for RR, RG, and GG that include the shadowing and spatial correlation for a specific factory environment was presented.

The proposed pathloss formula can be used to model any existing pathloss model up to this time. In this paper, Hata model for urban area and COST 231 Walfish-Ikegami in LOS and NLOS microcell are used in comparison with our model. The results show that our model fits better to the raw data (data from ray-tracing which is considered as the most accurate and reliable in prediction of the pathloss) than any models, including Free space and d^{-n} law.

With the propose spatial correlation formula, it is very easy to generate any correlated channel matrix compared to other methods because this formula requires only the basic proprieties such as the antenna size, antenna separation, and Rician K factor. We also note that this formula can be used in any environment and frequency. Only one parameter that characterizes the environment is K .

For a chosen factory environment, the Rician K factor is found to be 0.85, which means that this factory environment can be considered as a LOS microcell. This conclusion is also confirmed with the result in Section 2 (distribution of the spatial correlation can be modeled as Rician or Gaussian, which means the channel must have the LOS components) and Section 3 (the second good result from the fitting method is COST 231 Walfish-Ikegami in LOS microcell).

With these formulae, we can perform a high level simulation for any system using MIMO technology, such as future WSN with accuracy and speed.

References

- [1] D. S. Baum, J. Hansen, J. Salo, and P. Kyösti, “An Interim Channel Model for Beyond-3G Systems: Extending the 3GPP Spatial Channel Model (SCM),” *Vehicular Technology Conference, VTC-2005, IEEE 61st*, Vol. 5, pp. 3132-3136, May-Jun. 2005.
- [2] J. M. Molina-Garcia-Pardo, A. Martinez-Sala, M. V. Bueno-Delgado, E. Egea-Lopez, L. Juan-Llacer, and J. Garcia-Haro, “Channel Model at 868 MHz for Wireless Sensor Networks in Outdoor Scenarios,” *International Workshop on Wireless Ad-hoc Networks, IWWAN2005*, May 2005.
- [3] K. Mizutani, K. Sakaguchi, Jun-ichi Takada, and K. Araki, “Development of MIMO-SDR Platform and its Application to Real-Time Channel Measurements,” *IEICE Trans. Commun.*, Vol. E89-B, pp. 3197-3207, Dec. 2006.
- [4] A. Giorgetti, M. Chiani, M. Shafi, and P. J. Smith, “Characterizing MIMO Capacity Under the Influence of Spatial/Temporal Correlation,” *Australian Communication Theory Workshop Proceeding, AusCTW03*, 2003.
- [5] Li-Chun Wang, and Yun-Huai Cheng, “Modelling and Capacity Analysis of MIMO Rician Fading Channels for Mobile-to-Mobile Communications,” *Vehicular Technology Conference, VTC-2005, IEEE 62nd*, Vol. 2, pp. 1279-1283, Sept. 2005.
- [6] S. Loyka, and G. Tsoulos, “Estimating MIMO System Performance Using the Correlation Matrix Approach,” *Communications Letters, IEEE*, Vol. 6, pp. 19-21, Jan. 2002.
- [7] K. Leng, K. Sakaguchi, and K. Araki, “Pathloss model for factory environment,” *ISMAC Conference*, Bangkok, Thailand, Jan. 2009.
- [8] T. D. Abhayapala, R. A. Kenney, and J. T. Y. Ho, “On capacity of multi-antenna wireless channels: Effects of antenna separation and spatial correlation,” *Proc. 3rd AusCTW*, 2002.
- [9] C. Oestges, “Validity of the Kronecker Model for MIMO Correlated Channels,” *Vehicular Technology Conference, VTC 2006, IEEE 63rd*, Vol. 6, pp. 2818-2822, May 2006.

- [10] Min-Goo Choi, Sung ho Chae, Byung-Tae Yun and S. O. Park, "Validity of Kronecker model at 3.805GHz Indoor measurement 4 by 4 MIMO system," *IEEE Antenna and Propagation Symposium 2008*, San Diego, America, July 5-12, 2008.
- [11] http://en.wikipedia.org/wiki/Hata-Model_for_Urban_Area
- [12] "Spatial channel model for Multiple Input Multiple Output (MIMO) simulations (Release 6)," <http://www.3gpp.org>
- [13] S. Loyka, and A. Kouki, "On the use of Jensen's inequality for MIMO channel capacity estimation," *Canadian Conf. on Electrical and Computer Engineering (CCECE 2001)*, pp. 475-480, Toronto, Canada, May 13-16, 2001.
- [14] T. M. Cover, and J. A. Thomas, "Elements of Information Theory," *John Wiley & Sons*, New York, 1991.
- [15] S. G. C. Fraiha, J. C. Rodrigues, R. N. S. Barbosa, H. S. Gomes, and G. P. S. Cavalcante, "An Empirical Model for Propagation-Loss Prediction in Indoor Mobile Communications Using The Padé Approximant," *Microwave and Optoelectronics, 2005 SBMO/IEEE MTT-S International Conference*, pp. 625-628, Jul. 2005.
- [16] X. Gao, J. Zhang, G. Liu, D. Xu, P. Zhang, Y. Lu, and W. Dong, "Large-scale Characteristics of 5.25 GHz Based on Wideband MIMO Channel Measurements," *Antennas and Wireless Propagation Letters, IEEE*, vol. 6, pp. 263-266, Dec. 2007.

SDR Forum in 2004 and 2005 respectively, and the Excellent Paper Award from IEICE Japan in 2005. His current research interests are in MIMO propagation measurement, MIMO communication system, and software defined radio. He is a member of IEEE.



Kiyomichi Araki was born in Nagasaki on January 7, 1949. He received a B.E. degree in electrical engineering from Saitama University, in 1971, and M.E. and Ph.D. degrees in physical electronics both from the Tokyo Institute of Technology, in 1973 and 1978, respectively. In 1973-1975, and 1978-1985, he was a Research Associate at the Tokyo Institute of Technology, and in 1985-1995 he was an Associate Professor at Saitama University. In 1979-1980 and 1993-1994 he was a visiting research scholar at the University of Texas, Austin and University of Illinois, Urbana, respectively. He is currently a Professor at the Tokyo Institute of Technology. His research interests are information security, coding theory, communication theory, circuit theory, electromagnetic theory, and microwave circuits, etc. He is a member of IEEE and Information Processing Society of Japan.



KY Leng was born in Battambang, Cambodia, on May 06, 1979. He received a B.E. degree in electrical engineering from the Institute of Technology of Cambodia, in 2001, and M.E. degree in electrical engineering from the Chulalongkorn University, Bangkok, Thailand in 2005. In 2001-2003 and 2005-2006, he was a lecturer at the Institute of Technology of Cambodia. From 2006 till now, he is a Ph.D student at the Tokyo Institute of Technology, Tokyo, Japan. His research interests are communication system, electronic and computer programming.



Kei Sakaguchi was born in Osaka, Japan, on November 27, 1973. He received a B.E. degree in electrical and computer engineering from the Nagoya Institute of Technology, Japan, in 1996, and a M.E. degree in information processing from the Tokyo Institute of Technology, in 1998. In 2000-2007, he was an Assistant Professor at the Tokyo Institute of Technology. He is currently an Associate Professor at the Tokyo Institute of Technology. He received the Young Engineer Awards both from IEICE Japan and IEEE AP-S Japan chapter in 2001 and 2002 respectively, the Outstanding Paper Award from